


# Localization and density of tertiary lymphoid structures associate with molecular subtype and clinical outcome in colorectal cancer liver metastases

Chong Zhang,<sup>1</sup> Xiang-Yu Wang,<sup>2</sup> Jie-Liang Zuo,<sup>3</sup> Xue-Fu Wang,<sup>4,5</sup> Xiao-Wen Feng,<sup>4,5</sup> Bo Zhang,<sup>2</sup> Yi-Tong Li,<sup>2</sup> Chen-He Yi,<sup>2</sup> Peng Zhang,<sup>2</sup> Xiao-Chen Ma,<sup>2</sup> Zhen-Mei Chen,<sup>2</sup> Yue Ma,<sup>2</sup> Jia-Hao Han,<sup>2</sup> Bao-Rui Tao,<sup>2</sup> Rui Zhang,<sup>2</sup> Tian-Qi Wang,<sup>1</sup> Li Tong,<sup>1</sup> Wang Gu,<sup>1</sup> Si-Yu Wang,<sup>1</sup> Xiao-Fei Zheng,<sup>1</sup> Wen-Kang Yuan,<sup>1</sup> Zi-Jie Kan,<sup>1</sup> Jie Fan,<sup>6</sup> Xiang-Yang Hu,<sup>7</sup> Jun Li,<sup>3</sup> Chao Zhang,<sup>1</sup> Jin-Hong Chen <sup>2</sup>

**To cite:** Zhang C, Wang X-Y, Zuo J-L, *et al*. Localization and density of tertiary lymphoid structures associate with molecular subtype and clinical outcome in colorectal cancer liver metastases. *Journal for ImmunoTherapy of Cancer* 2023;11:e006425. doi:10.1136/jitc-2022-006425

► Additional supplemental material is published online only. To view, please visit the journal online (<http://dx.doi.org/10.1136/jitc-2022-006425>).

CZ, X-YW, J-LZ and X-FW contributed equally.

Accepted 18 January 2023



© Author(s) (or their employer(s)) 2023. Re-use permitted under CC BY-NC. No commercial re-use. See rights and permissions. Published by BMJ.

For numbered affiliations see end of article.

## Correspondence to

Dr Jin-Hong Chen;  
jinhongch@hotmail.com

Dr Chao Zhang;  
13965053990@163.com

Dr Jun Li; lijundfgd1@163.com

## ABSTRACT

**Background** Tertiary lymphoid structures (TLSs) have been proposed to assess the prognosis of patients with cancer. Here, we investigated the prognostic value and relevant mechanisms of TLSs in colorectal cancer liver metastases (CRCLM).

**Methods** 603 patients with CRCLM treated by surgical resection from three cancer centers were included. The TLSs were categorized according to their anatomic subregions and quantified, and a TLS scoring system was established for intratumor region (T score) and peritumor region (P score). Differences in relapse-free survival (RFS) and overall survival (OS) between groups were determined. Multiplex immunohistochemical staining (mIHC) was used to determine the cellular composition of TLSs in 40 CRCLM patients.

**Results** T score positively correlated with superior prognosis, while P score negatively associated with poor survival (all  $p < 0.05$ ). Meanwhile, T score was positively associated with specific mutation subtype of KRAS. Furthermore, TLSs enrichment gene expression was significantly associated with survival and transcriptomic subtypes of CRCLM. Subsequently, mIHC showed that the densities of Treg cells, M2 macrophages and Tfh cells were significantly higher in intratumor TLSs than in peritumor TLSs ( $p = 0.029$ ,  $p = 0.047$  and  $p = 0.041$ , respectively), and the frequencies of Treg cells and M2 macrophages were positively correlated with P score, while the frequencies of Tfh cells were positively associated with T scores in intratumor TLSs (all  $p < 0.05$ ). Next, based on the distribution and abundance of TLSs, an Immune Score combining T score and P score was established which categorized CRCLM patients into four immune classes with different prognosis (all  $p < 0.05$ ). Among them, patients with higher immune class have more favorable prognoses. The C-index of Immune Class for RFS and OS was higher than Clinical Risk Score statistically. These results were also confirmed by the other two validation cohorts.

**Conclusions** The distribution and abundance of TLSs is significantly associated with RFS and OS of CRCLM patients, and a novel immune class was proposed for predicting the prognosis of CRCLM patients.

## WHAT IS ALREADY KNOWN ON THIS TOPIC

⇒ Tertiary lymphoid structures (TLSs) provide a vital microenvironment for cellular immune response and are regarded as a predictor for evaluating the prognosis of patients with cancer. However, the mechanism of TLSs is not shown for prognostication of colorectal cancer liver metastases patients (CRCLMs).

## WHAT THIS STUDY ADDS

⇒ We demonstrate that increased T score, accompanied by elevated level of CD4<sup>+</sup>PD-1<sup>+</sup> Tfh cells, correlated with superior prognosis, while increased P score, accompanied by enhanced level of CD4<sup>+</sup>Foxp3<sup>+</sup> Treg cells and CD68<sup>+</sup>CD163<sup>+</sup> M2 macrophages, associated with poor survival. We further show that intratumor TLS infiltration is significantly associated with both transcriptomic subtype and mutational subtype of CRCLM. Also, we report that the immune class, established by combining T score and P score, is more diagnostic than Clinical Risk Score system in predicting the prognosis of CRCLMs.

## HOW THIS STUDY MIGHT AFFECT RESEARCH, PRACTICE OR POLICY

⇒ The findings indicate the superior prognostic value of TLSs, which could be exploited in future clinical practice.

## INTRODUCTION

Colorectal cancer (CRC) is the third most commonly diagnosed malignancy and has risen to the second leading cause of cancer-related death worldwide.<sup>1 2</sup> The prognosis of CRC is poor when metastasizing to the liver, which is the most frequent site of distant metastases.<sup>3–5</sup> The currently available multidisciplinary treatment strategies for CRC liver

metastases (CRCLM) have limited efficacy, and surgical resection is the only potential curative therapeutic option, despite 50%–75% of patients develop a recurrence within 2 years.<sup>6,7</sup> Several studies have shown a critical role of the immune microenvironment in the progression of CRCLM.<sup>8–10</sup> Therefore, it is necessary to investigate the characterization of immune contexture to evaluate its effect on the prognosis of CRCLM patients (CRCLMs).

Recently, the success of immunotherapy in various cancers emphasizes the need to better comprehend the mechanisms that lead to effective antitumoral responses.<sup>11,12</sup> Intratumoral T cells and B cells infiltration has been extensively explored and is correlated with favorable prognosis in most tumors.<sup>13,14</sup> Our previous study demonstrated that intratumor T cells were positive associated with a good prognosis of CRCLMs.<sup>3</sup> Meanwhile, several studies have focused on the significance of tertiary lymphoid structures (TLSs), an analog of secondary lymphoid organs, which are classically defined as lymphoid aggregates forming in sites of inflammation where autoimmune disease, infection and cancer exist.<sup>15,16</sup> TLSs are thought to provide an important microenvironment for both humoral and cellular antitumor-specific immune responses by providing sites for local antigen presentation and allowing the production of effector and central memory T cells.<sup>17,18</sup> The presence of intratumor TLSs is correlated with a decreased risk of recurrence and improved survival in most solid tumor, despite some conflicting results.<sup>13,19–21</sup> However, the prognostic value and clinical outcome of TLSs in CRCLMs remain unknown.

Thus, the purpose of this study is to investigate, by means of evaluating the spatial distribution, abundance and composition of TLSs, the prognostic value of both intratumor and peritumor TLSs in CRCLMs using three independent patient cohorts from different cancer centers. A novel TLS scoring system was established and used to evaluate the abundance of TLSs in the areas of intratumor, invasive margin and peritumor, uncovering the contrary prognostic roles of intratumor and peritumor TLSs, which explored by multiplex immunohistochemical staining (mIHC) to determine the cellular composition of TLSs. An immune class combining intratumor and peritumor TLS scores was established and defined four CRCLMs groups with significantly different prognoses.

## MATERIAL AND METHODS

### Patients and samples

This study included 603 CRCLMs from three different cancer centers who underwent curative surgery. The discovery cohort (HSH Cohort) contained 402 CRCLMs at Huashan Hospital Fudan University between 2014 and 2019. The validation cohort (TPH cohort) contained 106 CRCLMs from the Tenth People's Hospital of Tongji University between 2014 and 2019 and the FAH Cohort contained 95 CRCLMs from the First Affiliated

Hospital of Anhui Medical University between 2015 and 2019. Patients with a history of autoimmune disease and treated with immunosuppressive drugs or molecular targeted drugs were excluded. All patients were routinely followed by using peripheral blood laboratory testing and imaging examination (CT scan or MRI). The Clinical Risk Score (CRS) proposed by Fong *et al* was evaluated accordingly.<sup>22</sup> In brief, one point for each criterion as follows: positive margin, extrahepatic disease, node-positive primary, disease-free interval from primary to metastases <12 months, number of hepatic tumors >1, largest hepatic tumor >5 cm, and carcinoembryonic antigen level >200 ng/mL.

### Pathological evaluation of TLSs

For each case in HSH, TPH and FAH Cohorts, slides were examined by two independent pathologists blinded to patient outcome. TLSs were assessed morphologically on H&E stained slides, which were scanned into whole slide images (WSIs) by using the Mantra Quantitative Pathology Workstation (PerkinElmer, Waltham, Massachusetts, USA), as described previously.<sup>18,23</sup> Briefly, according to the maturation stages, TLSs were classified as<sup>18</sup>: (1) Aggregates (Agg): vague clusters of lymphocytes; (2) lymphoid follicles I (Fol-I): lymphoid follicles without germinal centers formation and (3) lymphoid follicles II (Fol-II): lymphoid follicles with germinal centers formation. Accordingly, CRCLMs were further classified according to the maturation of intratumor TLSs (the TLSs Maturation Class) as: (1) TLS<sup>negative</sup> CRCLM: tumors without intratumor TLSs; (2) Agg CRCLM: tumors with only Agg and without Fol-I or Fol-II; (3) Fol-I CRCLM: tumors with at least Fol-I, with or without Agg and without Fol-II and (4) Fol-II CRCLM: tumors with at least one Fol-II, with or without Agg without Fol-I.

To assess the spatial distribution of TLSs, all WSIs were divided into three subregions: intratumor (T), invasive margin (IM, area of 0.5 mm width between intratumor and peritumor<sup>24</sup> and peritumor (P) (online supplemental figure 1A). The TLS scoring system was established based on the abundance of TLSs in different subregions. In the T region (T score), TLS abundance was divided into four groups: (1) score 0: without TLS in the T region; (2) score 1: one or two TLSs in the T region; (3) score 2: more than two TLSs in the T region but does not converge with each other and (4) score 3: extensive TLSs in the T region and converges with each other. Similarly, TLS abundance was also divided into another four groups in the P region (P score): (1) score 0: without TLS in the P region; (2) score 1: the area of TLSs in the P region is less than 50%; (3) score 2: the area of TLSs in the P region is more than 50% and (4) score 3: extensive TLSs in the P region and converges with each other. TLS abundance in the IM region (IM score) was divided into three groups shown in online supplemental methods and figure 1B. Meanwhile, the degree of TLSs maturation stages was also assessed. Representative WSIs for TLS scoring system are shown in figure 1A.

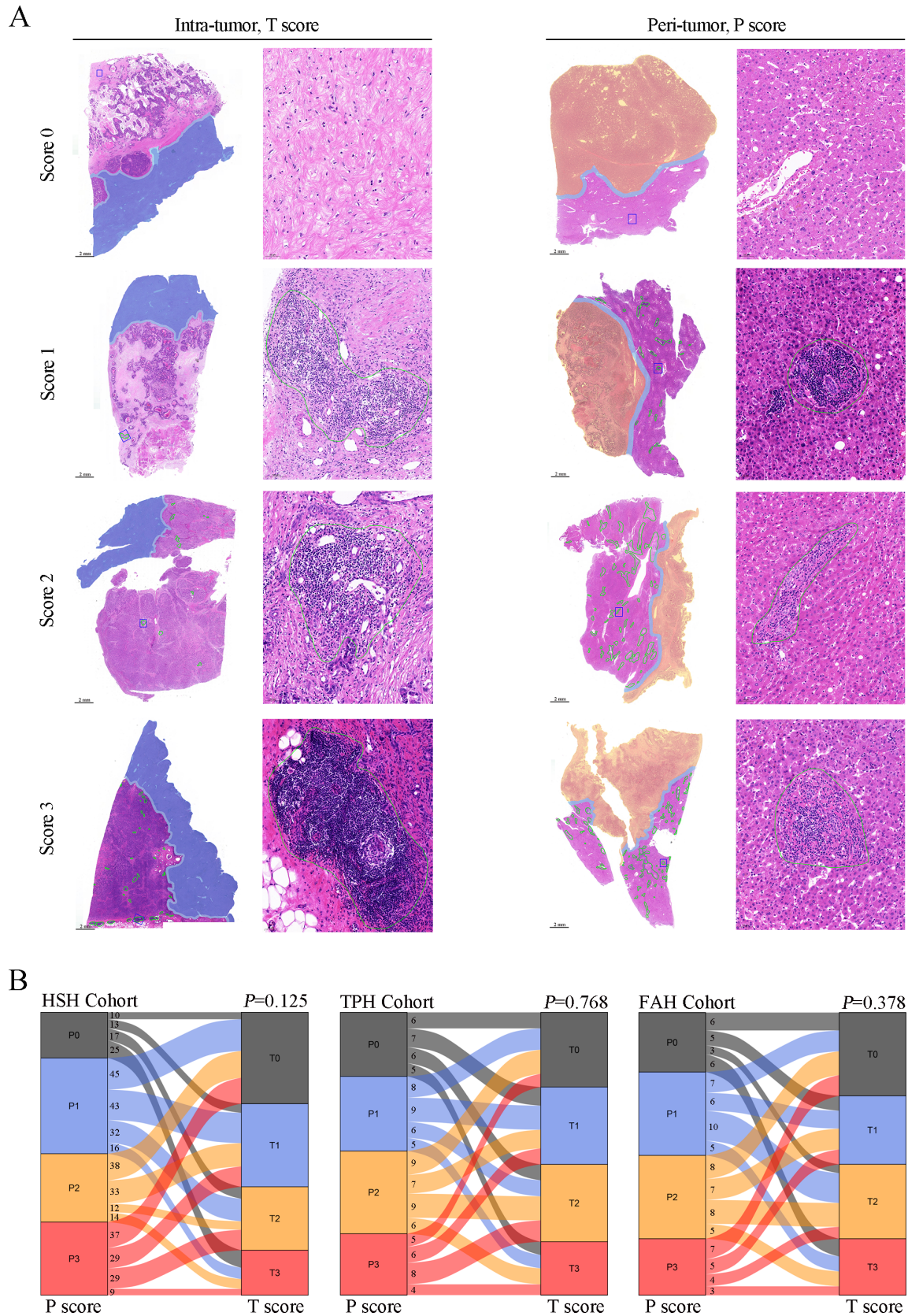


**Figure 1** Correlation between T score and P score. (A) Representative whole slide images of H&E staining for TLS scoring system (T and P scores). TLSs in intratumor and peritumor region were marked in green. Intratumor region (T score) was highlighted in light orange, while peritumor region (P score) was highlighted in deep blue. Invasive margin was highlighted in light blue. (B) No significant differences were showed between T score and P score for HSH, TPH and FAH Cohorts, respectively (all  $p>0.05$ ). TLS, tertiary lymphoid structures; HSH, Huashan Hospital Fudan University; TPH, Tenth People's Hospital of Tongji University; FAH, First Affiliated Hospital of Anhui Medical University.

To ensure the accuracy of TLS scoring system, the TLS fraction (area of TLSs/area of the scoring subregion) was calculated in HSH Cohort and the results showed that TLS scoring system could represent the abundance of TLSs (online supplemental figure 1C and D). Then, the TLS score in HSH, TPH and FAH Cohorts was assessed and the higher score was adopted when a slide got different scores from two independent pathologists (online supplemental figure 1E–G). Additional information on the TLS scoring system is shown in online supplemental methods.

### Gene expression profiling

The presence of TLSs could be evaluated by a 12-gene expression signature, as previously described, including CCL2, CCL3, CCL4, CCL5, CCL8, CCL18, CCL19, CCL21, CXCL9, CXCL10, CXCL11 and CXCL13.<sup>24</sup> We retrieved the gene expression profile data including 171 CRCLM samples from Gene Expression Omnibus (accession number GSE159216), analyzed on Affymetrix Human Transcriptome 2.0 Arrays. Clinical annotations have been downloaded for further analysis. For each sample, we calculated the geometric mean of the above 12 genes. Subsequently, sample with a geometric mean superior to the third quartile were classified as TLS+, while sample with a geometric mean inferior to the third quartile were classified as TLS-. The associations between TLS positivity with molecular subtype and clinical outcome were analyzed.

### mIHC and data analysis

mIHC was performed using the Opal 7-color IHC kit (PerkinElmer) as previously described.<sup>25</sup> Briefly, FFPE sections (4 μm thick) were dewaxed and rehydrated. Antigen retrieval was performed in citrate buffer (PH=6.0), and endogenous peroxidase was quenched using 3% H<sub>2</sub>O<sub>2</sub> for 15 min. The slides were blocked with 2% bovine serum albumin for 15 min and then incubated with primary antibodies of two panels overnight, including CD3, CD4, CD20, Foxp3 and PD-1; CD8, CD56, CD68, CD163 and PD-L1 (online supplemental table 1). Then, slides were incubated with corresponding HRP-conjugated secondary antibodies and fluorescent dyes with the following order: Opal540, Opal570, Opal620, Opal650 and Opal690 (PerkinElmer). Nuclei was stained with DAPI (PerkinElmer). Subsequently, the slides were scanned and imaged using the Mantra Quantitative Pathology Workstation (PerkinElmer, Waltham, Massachusetts, USA). Images were obtained for the following analysis using the inForm Advanced Image Analysis software (V.2.4.2, PerkinElmer). Multispectral images were unmixed using spectral libraries obtained from images of single-stained slides for each marker. For subregions with multiple TLSs, the densities and frequencies of each marker were averaged to represent the cellular composition.

### Statistical analysis

Statistical analysis was performed using SPSS software V.23.0 (IBM). Categorical variables were assessed with the  $\chi^2$  test or Fisher's exact test. Continuous variables were assessed with the Student's t-test or Mann-Whitney U test, and were summarized as the mean with SD or medians and IQR. The association between two continuous variables was assessed by Pearson's correlation coefficient. Survival curves were analyzed by the Kaplan-Meier method and log-rank test. Univariable and multivariable Cox regression analysis were performed to evaluate independent factors associated with relapse-free survival (RFS) and overall survival (OS). The results of Cox regression analysis were presented as HR with 95% CIs. The predictive performance of different staging systems was measured using Harrell's concordance index (C-index). A two-sided  $p < 0.05$  was considered statistically significant.

## RESULTS

### Clinicopathological characteristics of CRCLMs

The clinical characteristics of the patients from three different cancer centers are presented in [table 1](#). A total of 603 CRCLMs were included, among whom 388 (64.3%) patients were men and the median age was 59 years (IQR 52–67 years). Up to June 2022, the mean follow-up time was 27.7 (range 0.2–136.7), 34.4 (range 0.8–86.8) and 24.2 (range 5.1–86.5) months for HSH, TPH and FAH cohorts, respectively. The median RFS time was 12.0 (range 0.2–93.2), 17.5 (range 0.8–86.8) and 14.3 (range 1.2–86.5) months for HSH, TPH and FAH Cohorts, respectively. The median OS time was 25.1 (range 0.2–136.7), 31.0 (range 0.8–86.8), and 23.1 (range 3.5–86.5) months for HSH, TPH, and FAH Cohorts, respectively. The percentage of patients with metachronous liver metastases was 32.8%, 39.6%, and 42.1%, while the percentage of patients with synchronous liver metastases was 67.2%, 60.4%, and 57.9% for HSH, TPH, and FAH cohorts, respectively. The median size of liver tumors was 4.5 cm (range 0.5–19 cm), 3.5 cm (range 0.3–15 cm) and 4.2 cm (range 0.5–17 cm) for HSH, TPH, and FAH cohorts, respectively. The median number of liver tumors was 2 (range 1–22), 2 (range 1–13), and 2 (range 1–8) for HSH, TPH and FAH Cohorts, respectively. The number of patients treated with neoadjuvant chemotherapy was 227, 58, and 44 for HSH, TPH and FAH cohorts, respectively.

### TLSs in different subregions are associated with different prognoses of CRCLMs

A number of patients with different T and P scores in three cohorts are shown in [figure 1B](#). Interestingly, there was no significant difference between T and P scores, suggesting the abundance of TLSs in different subregions was independent of each other (all  $p > 0.05$ ).

The TLS scores in three different subregions in HSH cohort were evaluated and showed obviously different prognostic values. T score was positively associated with RFS and OS, significantly ([figure 2A](#), all  $p < 0.001$ ), while

**Table 1** Clinicopathologic characteristics of CRCLM patients underwent liver resection

Characteristic	HSH cohort	TPH cohort	FAH cohort	P value	P value
	(n=402)	(n=106)	(n=95)	(HSH vs TPH)	(HSH vs FAH)
Sex (%)					
Male	264 (65.7)	66 (62.3)	58 (61.1)	0.513	0.397
Female	138 (34.3)	40 (37.7)	37 (38.9)		
Age (years)					
Mean (SD)	59.4 (11.4)	57.3 (12.2)	58.3 (12.3)	0.112	0.406
Range	(25.0–86.0)	(25.0–82.0)	(31.0–84.0)		
Occurrence of metastases (%)					
Metachronous	132 (32.8)	42 (39.6)	40 (42.1)	0.190	0.088
Synchronous	270 (67.2)	64 (60.4)	55 (57.9)		
Primary tumor location (%)					
Left-sided	300 (74.6)	73 (68.9)	66 (69.5)	0.323	0.305
Right-sided	102 (25.4)	33 (31.1)	29 (30.5)		
CEA (ng/mL)					
Mean (SD)	67.8 (278.9)	121.0 (393.9)	210.2 (590.7)	0.193	0.024
Range	(0.5–4762.0)	(0.7–3367.0)	(0.6–3181)		
CA19-9 (U/mL)					
Mean (SD)	149.0 (559.4)	117.0 (294.1)	228.8 (578.9)	0.562	0.215
Range	(0.6–6175.0)	(2.4–1924.0)	(0.8–3164)		
CA125 (U/mL)					
Mean (SD)	82.0 (342.0)	75.9 (302.2)	201.3 (632.3)	0.867	0.078
Range	(1.9–5721.0)	(2.5–3015.0)	(0.7–3751)		
Size (cm) (%)					
<5	317 (78.9)	74 (69.8)	70 (73.7)	0.049	0.275
≥5	85 (21.1)	32 (30.2)	25 (26.3)		
Tumor no (%)					
Single	177 (44.0)	44 (41.5)	34 (35.8)	0.641	0.144
Multiple	225 (56.0)	62 (58.5)	61 (64.2)		
Liver fibrosis (%)					
Yes	40 (10.0)	22 (20.8)	14 (14.7)	0.003	0.178
No	362 (90.0)	84 (79.2)	81 (25.3)		
Tumor grade (%)					
G1-2	302 (75.1)	72 (67.9)	70 (73.7)	0.135	0.771
G3	100 (24.9)	34 (32.1)	25 (26.3)		
T stage (%)					
Tis-2	311 (77.4)	51 (48.1)	70 (73.7)	<0.001	0.446
T3-4	91 (22.6)	55 (51.9)	25 (26.3)		
Lymph node metastasis (%)					
Yes	292 (72.6)	64 (60.4)	57 (60.0)	0.014	0.015
No	110 (27.4)	42 (39.6)	38 (40.0)		
CRS (%)					
Low (0–2)	253 (62.9)	70 (66.0)	61 (64.2)	0.555	0.817
High (3–5)	149 (37.1)	36 (34.0)	34 (35.8)		
Differentiation (%)					

Continued

**Table 1** Continued

Characteristic	HSH cohort (n=402)	TPH cohort (n=106)	FAH cohort (n=95)	P value (HSH vs TPH)	P value (HSH vs FAH)
Poor	97 (24.1)	22 (20.8)	15 (15.8)	0.475	0.208
Moderate	197 (49.0)	59 (55.7)	53 (55.8)		
Well	108 (26.9)	25 (23.5)	27 (28.4)		
Gene status (%)					–
Wild-type	211 (52.5)	47 (44.3)	–	0.064	–
KRAS mutant	114 (28.3)	31 (29.3)	–		
NRAS mutant	12 (3.0)	7 (6.6)	–		
BRFA mutant	4 (1.0)	5 (4.7)	–		
Unknown	61 (15.2)	16 (15.1)	–		
Neoadjuvant chemotherapy (%)					
Yes	227 (56.5)	58 (54.7)	44 (46.3)	0.747	0.074
No	175 (43.5)	48 (45.3)	51 (53.7)		

CEA, carcinoembryonic antigen; CRCLM, colorectal cancer liver metastases; CRS, Clinical Risk Score; FAH, First Affiliated Hospital of Anhui Medical University; HSH, Huashan Hospital Fudan University; TPH, Tenth People's Hospital of Tongji University.

the P score was negatively correlated with RFS and OS (figure 2B, all  $p < 0.001$ ), significantly. Furthermore, we also evaluated the maturation stages of TLSs in HSH Cohorts and demonstrated that no significant association was found between the subregion and maturation stages of TLSs (online supplemental figure 1H),  $p = 0.756$ ). Also, we found that CRCLMs with Fol had a significantly prolonged RFS and OS than CRCLMs with TLS<sup>negative</sup> and Agg (online supplemental figure 1I and J, all  $p < 0.001$ ), which suggested the maturation stages of intratumor TLSs has a prognostic impact on CRCLM. Meanwhile, we found that this TLS maturation classification was positively correlated with the T score, significantly (online supplemental figure 1K,  $p < 0.001$ ), and was as an independent prognostic factor of RFS and OS in univariate and multivariate analysis (online supplemental table 2 and 3, all  $p < 0.05$ ). Conversely, we found that there was no correlation between RFS and OS of CRCLMs and IM score (online supplemental figure 1L and M,  $p = 0.326$  and  $0.913$ , respectively). Therefore, the IM score was excluded in the subsequent analysis. Meanwhile, these findings were also confirmed in the TPH and FAH cohorts, where higher T score, in contrast to P score, was significantly correlated with increased RFS and OS (figure 2C–F, all  $p < 0.05$ ). Furthermore, the prognostic value of a TLSs gene expression signature was further validated in the public data of GSE159216 (figure 2G), and we found that samples with TLS+ has a significantly more favorable prognosis than samples with TLS– (figure 2H).

#### The association of TLSs with clinicopathological factors and molecular subtype

We first analyzed the correlation between TLS scores and clinicopathological characteristics of CRCLMs in the HSH and TPH cohorts. As shown in online supplemental table 4, the T score was negatively correlated with CEA serum

level, CA19-9 serum level, tumor size, tumor number, tumor grade, T stage and lymph node metastasis, while the P score was positively correlated with CA19-9 serum level (all  $p < 0.05$ ). The different clinicopathological correlations and opposite prognostic values between T and P scores suggested a crucial difference between intratumor and peritumor TLSs. These data suggest the possibility that a high T score is positively correlated with activation of the immune microenvironment, while a high P score is negatively correlated with activation of the immune microenvironment. Next, we investigated the correlation between the TLS enrichment gene signature and a previously proposed liver metastasis subtype (LMS) system recapitulated the main distinction between epithelial-like and mesenchymal-like tumors, with abundant immune and stromal component.<sup>26</sup> We found that TLS enrichment gene signature was significantly associated with LMS (figure 2I,  $p < 0.001$ ), which showed that samples with LMS5 have a more favorable prognosis than those with LMS1 (figure 2J).

The relationship between TLS infiltration and gene mutations of BRAF, KRAS and NRAS in the HSH and TPH cohorts was also examined, and we found that no consistently significant correlation across the cohorts (online supplemental figure 2A–C). Also, the gene mutations of KRAS, NRAS and TP53 within T region in GSE159216 were not significantly associated with TLS enrichment (online supplemental table 5). Subsequently, the specific site of KRAS mutation was further investigated and we found that except for KRAS G12S mutation, KRAS G12A, G12C, G12D, G12R, G12V, G13C and G13D mutations were significantly correlated with T score, which demonstrated immune subtypes correlated with common gene mutations (figure 2K). The results demonstrated that the specific subtypes of KRAS gene mutations might have an influence on the tumor immune microenvironment.

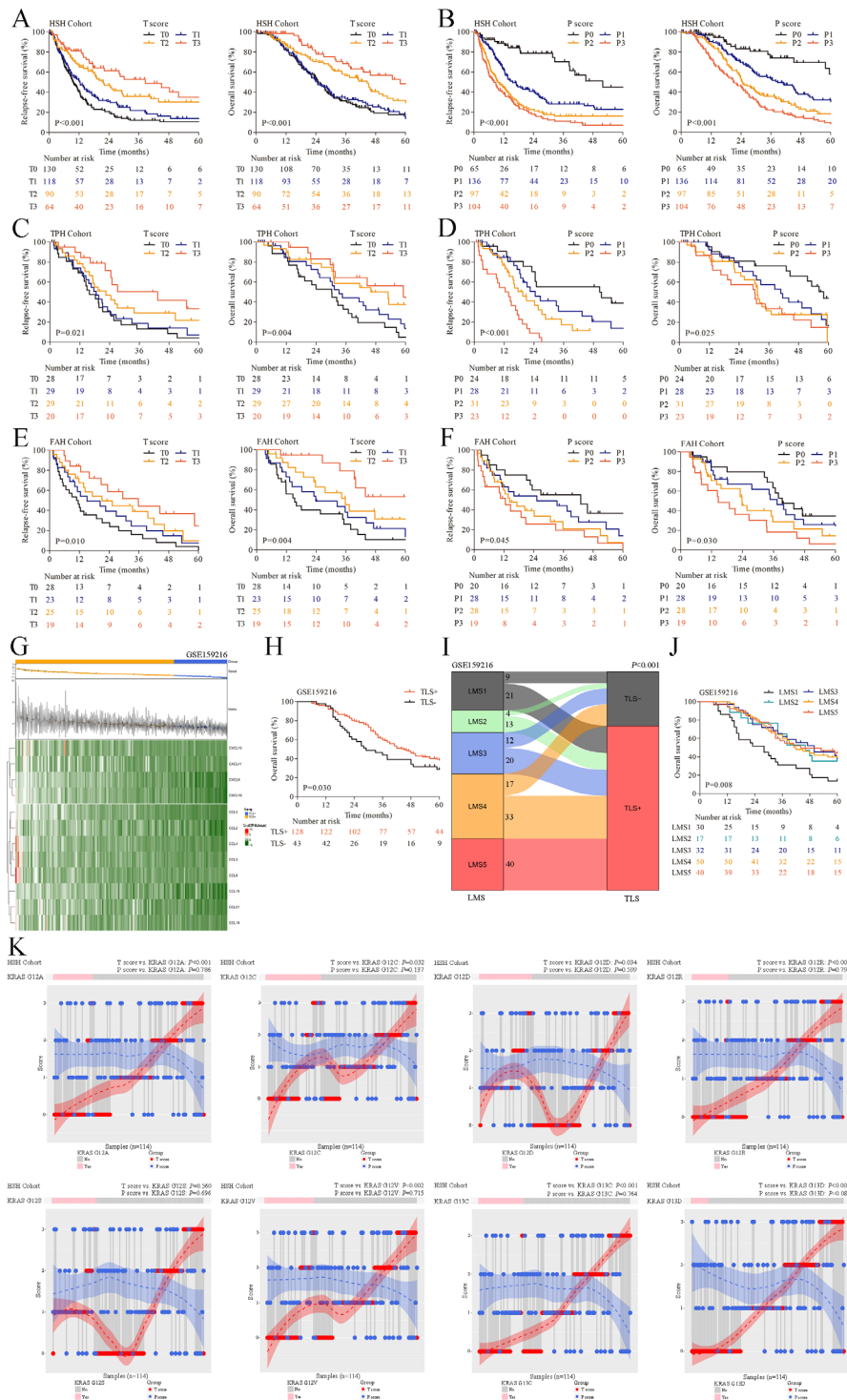


**Figure 2** Prognostic value of T and P scores in CRCLM patients and correlation between gene mutation and T and P scores. (A, B) Kaplan-Meier curves showing relapse-free survival (RFS) and overall survival (OS) of CRCLM patients stratified by T score (A) and P score (B) in the HSH Cohort, respectively. (C, D) Kaplan-Meier curves showing RFS and OS of CRCLM patients stratified by T score (C) and P score (D) in the TPH Cohort, respectively. (E, F) Kaplan-Meier curves showing RFS and OS of CRCLM patients stratified by T score (E) and P score (F) in the FAH Cohort, respectively. (G) Heat map of TLS relative gene expression in GSE159216. (H) Kaplan-Meier curves showing OS of CRCLM patients stratified by TLS infiltration. (I) Significant correlations between TLS infiltration and LMS. (J) Kaplan-Meier curves showing OS of CRCLM patients stratified by LMS. (K) Relevance of T score and P score to gene mutation in the HSH Cohort. The pick represents a mutation of gene, while the gray represents a wild-type of gene at the top. The connected red and blue circles on each column represent a patient's T score and P score, respectively. The red and blue curves represent the overall distribution of T score and P score of patients, respectively. CRCLM, colorectal cancer liver metastases; LMS, liver metastasis subtype; TLSs, tertiary lymphoid structures; HSH, Huashan Hospital Fudan University; TPH, Tenth People's Hospital of Tongji University; FAH, First Affiliated Hospital of Anhui Medical University.

### The levels of immune cell composition in TLSs in different subregions

To explore the underlying mechanisms for the opposite prognostic value of intratumor and peritumor TLSs, we first included 20 CRCLM samples from the HSH Cohort, and stained the sections by H&E and mIHC, respectively (figure 3A). Detailed clinical characteristics and relative TLS scoring information are shown in online supplemental table 6. Then, the association between TLS score and immune cell composition was analyzed. Of the seven types of immune cells, including Th cells (CD3<sup>+</sup>CD4<sup>+</sup>), cytotoxic T lymphocytes (CD3<sup>+</sup>CD8<sup>+</sup>), Tfh cells (CD4<sup>+</sup>PD-1<sup>+</sup>), Treg cells (CD4<sup>+</sup>Foxp3<sup>+</sup>), B cells (CD20<sup>+</sup>), NK cells (CD56<sup>+</sup>) and macrophages (CD68<sup>+</sup>) (figure 3B), the distribution of Treg cell, M2 macrophages and Tfh cells was significantly different between intratumor and peritumor TLSs. The densities and frequencies of CD4<sup>+</sup>Foxp3<sup>+</sup> Treg cells and CD4<sup>+</sup>PD-1<sup>+</sup> Tfh cells among CD4<sup>+</sup> T cells and CD68<sup>+</sup>CD163<sup>+</sup> M2 macrophages among CD68<sup>+</sup> macrophages were significantly elevated in intratumor TLSs, compared with peritumor TLSs (figure 3C,D, density: Treg cells,  $p=0.029$ , Tfh cells,  $p=0.041$ , M2 macrophages,  $p=0.047$ ; frequency: Treg cells,  $p=0.006$ , Tfh cells,  $p=0.009$ , M2 macrophages,  $p=0.035$ ). However, compared with peritumor TLSs, the density and frequency of the other types of immune cells, including of CD20<sup>+</sup> B cells, CD8<sup>+</sup> cytotoxic T lymphocytes, CD56<sup>+</sup> NK cells and CD68<sup>+</sup> macrophages, showed no significant differences in intratumor TLSs (online supplemental figure 3A,B). Then, we found that the frequency of Treg cells and M2 macrophages in intratumor TLSs decreased significantly among T scores of 1–3 and increased significantly among P scores of 0–3 (figure 3E–G), indicating a potential association between peritumor TLS abundance and intratumor immunosuppressive microenvironment. On the contrary, the frequency of Tfh cells increased significantly in intratumor TLSs among T scores of 0–2 (figure 3E,F), suggesting the positive balance of immune microenvironment in intratumor TLSs. Meanwhile, we found that the densities of CD8<sup>+</sup> cytotoxic T lymphocytes in intratumor TLSs enhanced, which accompanied by the T score, while the densities of CD68<sup>+</sup> macrophages and PD-L1<sup>+</sup> cells decreased (online supplemental figure 3D). However, the densities of CD20<sup>+</sup> B cells decreased along with P score and did not associate with T score (online supplemental figure 3C,E). The densities of other types of immune cells, consisting of CD3<sup>+</sup>, CD4<sup>+</sup> and CD56<sup>+</sup> cells in intratumor and peritumor TLSs, associated with neither the T score nor P score (online supplemental figure 3C–F). These results were further verified by TPH Cohort with 20 CRCLM samples (online supplemental table 6 and figure 4).

### An immune class combining the T score and P score

To further investigate the opposite roles of the T score and P score in predicting the prognosis of CRCLM, an Immune Score combining T score and P score was established. The T score and P score was weighted by a

regression coefficient derived from a multivariate Cox regression analysis of RFS and OS which was transformed into the following formula in HSH Cohort: Immune Score (RFS) = (0.52×T score) + (−0.77×P score), Immune Score (OS) = (0.67×T score) + (−0.90×P score) (online supplemental table 7). In these formulas, the positive coefficient represents a protective factor, while the negative coefficient represents a risk factor. Then, based on the Immune Score, CRCLM patients were categorized into immune class I, II, III, and IV (online supplemental table 7), which represented the distribution and abundance of TLSs. CRCLM patients in immune class I showed TLSs mainly located in the P region, while patients in immune class IV showed TLSs primarily located in the T region. CRCLM patients in immune class II and III revealed different distributions and abundances of TLSs located in the T and P regions.

In the HSH, TPH and FAH cohorts, the CRCLM patients in the four immune classes had significant differences of RFS and OS (figure 4A–F, all  $p<0.05$ ). Multivariate Cox analysis demonstrated that immune class was an independent risk factor for RFS and OS among all three cohorts (tables 2 and 3, all  $p<0.05$ ). Compared with immune class I, the patients in immune class IV had significantly superior RFS and OS. Patients in immune class IV were at the lowest risk, with median RFS time of 18.5 months (95% CI 22.1 to 32.8 months), 48.3 months (95% CI 31.3 to 54.7 months) and 29.5 months (95% CI 26.0 to 46.5 months) and median OS time of 26.7 months (95% CI 28.2 to 41.3 months), 55.6 months (95% CI 38.7 to 60.8 months) and 39.9 months (95% CI 33.5 to 51.6 months) for HSH, TPH and FAH Cohorts, respectively. However, patients in immune class I were at the highest risk, with median RFS time of 7.9 months (95% CI 10.3 to 14.8 months), 13.2 months (95% CI 9.5 to 17.0 months) and 9.0 months (95% CI 7.7 to 22.3 months) and median OS time of 22.3 months (95% CI 22.2 to 27.8 months), 30.4 months (95% CI 20.1 to 33.8 months) and 11.1 months (95% CI 11.3 to 26.6 months) for HSH, TPH, and FAH cohorts, respectively.

To verify the diagnostic accuracy of the immune class in predicting RFS and OS of CRCLM patients, the C-index of the immune class and CRS was assessed, and we found that the C-index of immune class for RFS prediction was 0.774 (95% CI 0.772 to 0.825), 0.760 (95% CI 0.659 to 0.861) and 0.715 (95% CI 0.558 to 0.872) and OS prediction was 0.801 (95% CI 0.756 to 0.846), 0.750 (95% CI 0.639 to 0.862) and 0.732 (95% CI 0.610 to 0.854) for HSH, TPH and FAH cohorts, respectively, which was higher than CRS (RFS: 0.683, 0.661 and 0.657; OS: 0.642, 0.610 and 0.605 for HSH, TPH and FAH cohorts, respectively).

### DISCUSSION

The immune microenvironment, over the past decade, has been extensively investigated because of the remarkable advances in immunotherapy.<sup>27 28</sup> The tumor stroma



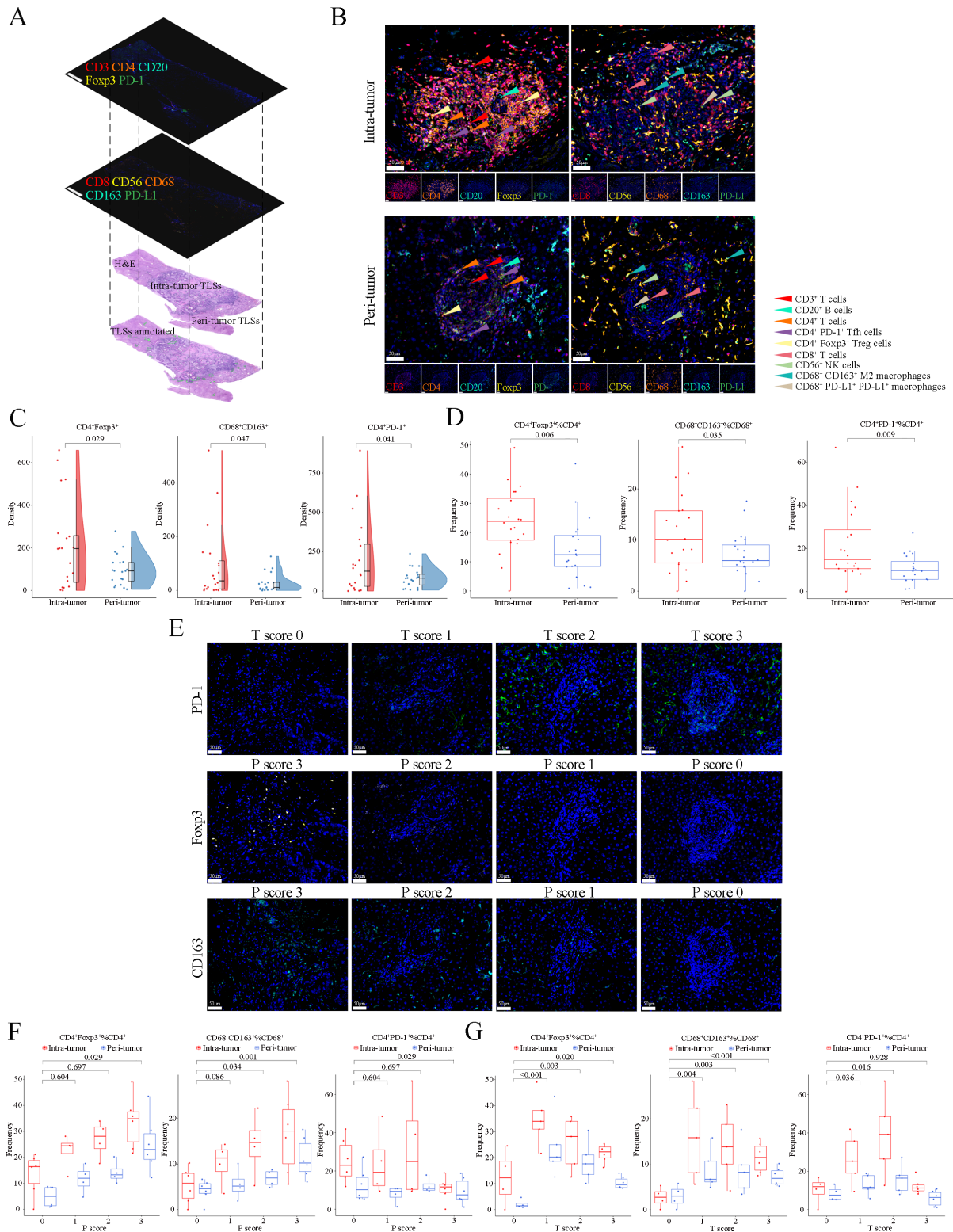


**Figure 3** The different distribution of Tfh cells, Treg cells and M2 macrophages in intratumor and peritumor TLSs. (A) H&E staining (including TLSs annotation) and mIHC staining (CD3, CD4, CD20, Foxp3 and PD-1; CD8, CD56, CD63, CD163 and PD-L1) images of TLSs were spatially matched in CRCLM patients. (B) Representative mIHC images showing the positive expression of CD3, CD4, CD20, Foxp3, PD-1, CD8, CD56, CD63, CD163 and PD-L1 in intratumor and peritumor TLSs. Scale bar, 50  $\mu$ m. (C, D) Quantification of the density (C) and frequency (D) of CD4<sup>+</sup>PD-1<sup>+</sup> Tfh cells, CD4<sup>+</sup>Foxp3<sup>+</sup> Treg cells and CD68<sup>+</sup>CD163<sup>+</sup> M2 macrophages in intratumor and peritumor TLSs. (E) Representative mIHC images showing the staining of PD-1, Foxp3 and CD163 in intratumor TLSs with different T score and P score. Scale bar, 50  $\mu$ m. (F, G) Quantification of the frequency of CD4<sup>+</sup>PD-1<sup>+</sup> Tfh cells and CD4<sup>+</sup>Foxp3<sup>+</sup> Treg cells within CD4<sup>+</sup> T cells and CD68<sup>+</sup>CD163<sup>+</sup> M2 macrophages within CD68<sup>+</sup> macrophages in intratumor and peritumor TLSs with different T score (F) and P score (G). mIHC, multiplex immunohistochemical staining; TLSs, tertiary lymphoid structures.

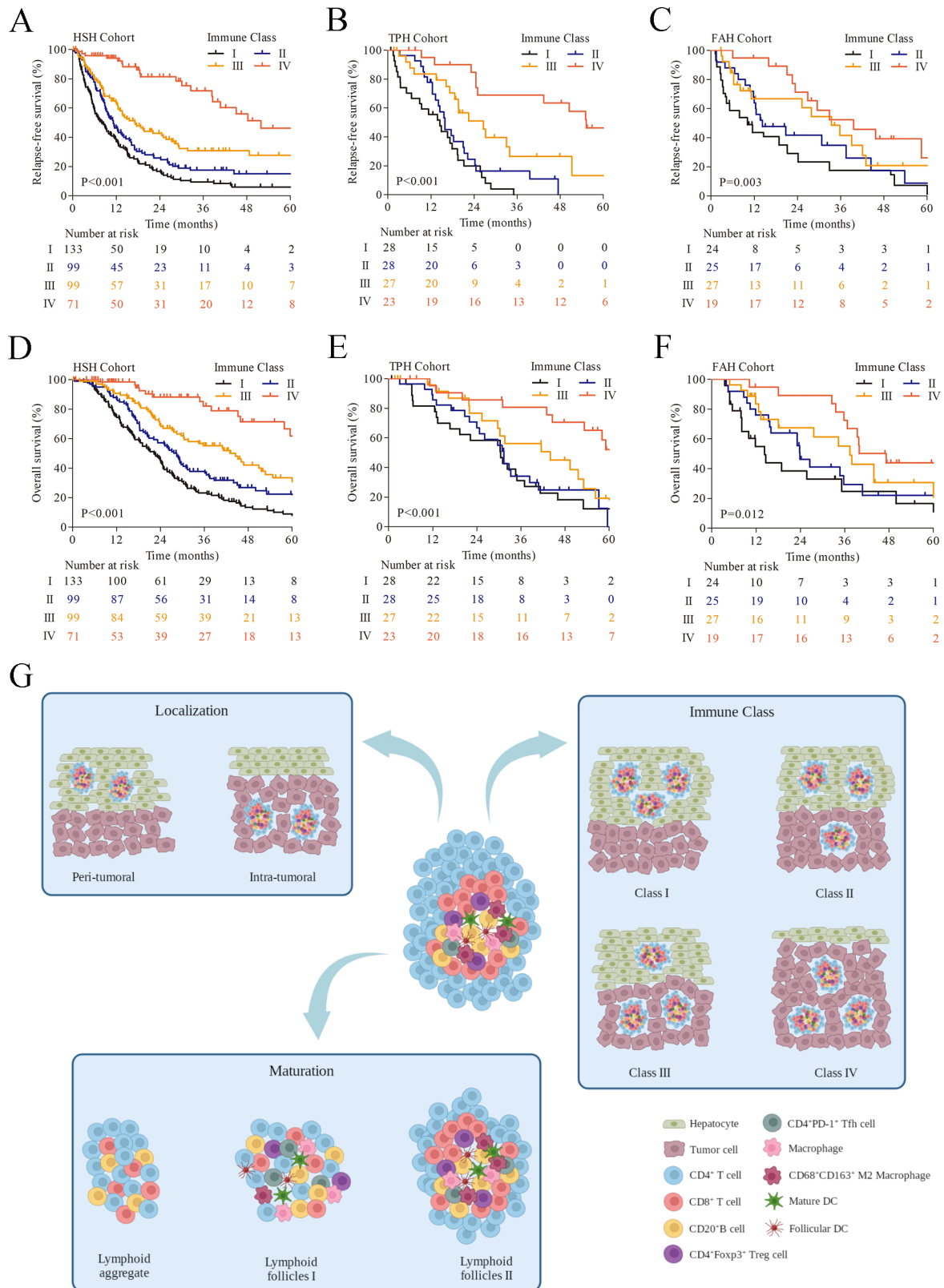


**Figure 4** An Immune Class combining the T score and P score and a schematic diagram of different Immune Class. (A) (A–C) Kaplan-Meier curves showing relapse-free survival of CRCLM patients stratified by Immune Class in the HSH Cohort (A), TPH Cohort (B) and FAH Cohort (C). (D–F) Kaplan-Meier curves showing overall survival of CRCLM patients stratified by Immune Class in the HSH Cohort (D), TPH Cohort (E) and FAH Cohort (F). (G) The schematic diagram created with Biorender.com showing the distribution and cellular compositions of TLSs in different Immune Class. CRCLM, colorectal cancer liver metastases; TLSs, tertiary lymphoid structures; HSH, Huashan Hospital Fudan University; TPH, Tenth People’s Hospital of Tongji University; FAH, First Affiliated Hospital of Anhui Medical University.

**Table 2** Multivariate analyses of factors associated with relapse-free survival in CRCLM patients

Variables	HSH cohort (n=402)		TPH cohort (n=106)		FAH cohort (n=95)	
	HR (95% CI)	P value	HR (95% CI)	P value	HR (95% CI)	P value
CEA (ng/mL) (5< vs ≥5)	1.432 (1.065 to 1.925)	0.018	1.297 (0.721 to 2.333)	0.386	2.299 (1.027 to 5.147)	0.043
CA19-9 (U/mL) (40< vs ≥40)	1.025 (0.787 to 1.334)	0.854	1.124 (0.667 to 1.895)	0.661	1.132 (0.685 to 1.872)	0.628
Size, cm (5< vs ≥5)	1.101 (0.789 to 1.537)	0.572	1.171 (0.616 to 2.225)	0.630	0.806 (0.444 to 1.463)	0.478
Tumor no (single vs multiple)	1.360 (1.061 to 1.745)	0.015	1.449 (0.787 to 2.670)	0.234	1.856 (1.045 to 3.298)	0.035
T stage (Tis-2 vs T3-4)	0.920 (0.657 to 1.289)	0.629	1.068 (0.606 to 1.881)	0.821	1.281 (0.722 to 2.271)	0.398
Lymph node metastasis (yes vs no)	1.345 (1.042 to 1.647)	0.024	0.868 (0.495 to 1.523)	0.622	2.578 (1.397 to 4.756)	0.002
Neoadjuvant chemotherapy (yes vs no)	1.275 (1.036 to 1.637)	0.044	1.192 (0.700 to 2.030)	0.518	2.369 (1.152 to 4.870)	0.019
Immune class		<0.001		0.001		0.007
Class I	Reference		Reference		Reference	
Class II	2.810 (1.676 to 4.712)	<0.001	3.305 (1.350 to 8.091)	0.009	2.348 (1.206 to 4.593)	0.011
Class III	3.926 (2.350 to 6.558)	<0.001	5.305 (2.176 to 12.930)	<0.001	2.743 (1.292 to 4.618)	0.009
Class IV	5.365 (3.258 to 8.835)	<0.001	7.294 (2.818 to 18.879)	<0.001	3.320 (1.442 to 7.642)	0.005

CEA, carcinoembryonic antigen; CRCLM, colorectal cancer liver metastases; FAH, First Affiliated Hospital of Anhui Medical University; HSH, Huashan Hospital Fudan University; TPH, Tenth People's Hospital of Tongji University.

is composed of an extracellular matrix including non-tumor cells of various lineages containing immune cells.<sup>29,30</sup> TLSs provide a vital microenvironment for the cellular immune response directed against tumor cells and are regarded as a predictor of a favorable prognosis in various solid cancers.<sup>13,16</sup> Several studies have indicated that consistent with tumor infiltrating lymphocytes, Crohn's disease-like lymphoid reaction characterized by peritumoral lymphoid aggregates was a common feature of high levels of microsatellite instability (MSI-H), and has also been associated with improved prognosis in CRC.<sup>31,32</sup> Further, Chang *et al*<sup>33</sup> showed that lymphocytic

infiltrate was associated with a survival benefit regardless of MSI status but did not note a survival difference between MSI-H tumors with a host immune response and microsatellite-stable tumors with a host immune response. In our study, we demonstrated the different role of TLSs based on distribution and density in CRCLM patients' tumors. The abundance of intratumor TLSs was an indicator of favorable clinical outcome for patients, while the location of peritumor TLSs was significantly correlated with a poor prognosis. Although the opposite role of TLSs in different region has been reported in hepatocellular carcinoma,<sup>34</sup> the underlying mechanism

**Table 3** Multivariate analyses of factors associated with overall survival in CRCLM patients

Variables	HSH cohort (n=402)		TPH cohort (n=106)		FAH cohort (n=95)	
	HR (95% CI)	P value	HR (95% CI)	P value	HR (95% CI)	P value
CEA (ng/mL) (5< vs ≥5)	1.334 (0.991 to 1.795)	0.058	2.576 (1.401 to 4.736)	0.002	1.588 (0.743 to 3.395)	0.233
Tumor no (single vs multiple)	1.324 (0.991 to 1.769)	0.058	2.047 (1.120 to 3.740)	0.020	1.829 (0.945 to 3.537)	0.073
Tumor grade (G1-2 vs G3)	1.202 (0.903 to 1.601)	0.208	1.167 (0.662 to 2.057)	0.593	1.431 (0.824 to 2.486)	0.204
T stage (Tis-2 vs T3-4)	0.940 (0.704 to 1.257)	0.678	0.631 (0.369 to 1.078)	0.092	1.251 (0.742 to 2.109)	0.401
Lymph node metastasis (yes vs no)	1.349 (1.037 to 1.754)	0.026	0.819 (0.464 to 1.443)	0.490	2.652 (1.453 to 4.843)	0.001
Neoadjuvant chemotherapy (yes vs no)	1.537 (1.176 to 2.008)	0.002	1.480 (1.075 to 1.975)	0.029	3.100 (1.714 to 5.606)	<0.001
Immune class		<0.001		<0.001		0.018
Class I	Reference		Reference		Reference	
Class II	2.384 (1.335 to 4.255)	<0.001	5.990 (2.264 to 15.845)	<0.001	1.708 (1.090 to 3.192)	0.037
Class III	3.590 (2.022 to 6.374)	<0.001	6.498 (2.577 to 16.387)	<0.001	2.771 (1.773 to 4.060)	0.021
Class IV	4.915 (2.805 to 8.613)	<0.001	8.409 (3.258 to 21.704)	<0.001	3.540 (2.136 to 5.679)	0.012

CEA, carcinoembryonic antigen; CRCLM, colorectal cancer liver metastases; FAH, First Affiliated Hospital of Anhui Medical University; HSH, Huashan Hospital Fudan University; TPH, Tenth People's Hospital of Tongji University.

also remain unknown. Here, the present study revealed that the frequency of CD4<sup>+</sup>Foxp3<sup>+</sup> Treg cells among CD4<sup>+</sup> T cells and CD68<sup>+</sup>CD163<sup>+</sup> M2 macrophages among CD68<sup>+</sup> macrophages was elevated significantly in intratumor TLSs, compared with peritumor TLSs. Meanwhile, the frequency of Treg cells and M2 macrophages was increased significantly in intratumor TLSs accompanied by the increasing level of those in peritumor TLSs, which indicated a potential association between peritumor TLSs and intratumor immunosuppressive microenvironment. However, compared with peritumor TLSs, the frequency of CD4<sup>+</sup>PD-1<sup>+</sup> Tfh cells among CD4<sup>+</sup> T cells was significantly higher in intratumor TLSs. Tfh cells play an important role in the formation of germinal centers to reconstruct the tumor microenvironment and promote the process of antitumor immune responses.<sup>35–37</sup> Therefore, the level of Tfh cells in intratumor TLSs are positively correlated with the prognosis of CRCLM patients.

A previous study demonstrated that the densities of Treg cells were significantly higher in recurrent tumors than in not-recurrent tumors, and a higher proportion of Treg cells could be one of the independent risk factors for recurrence.<sup>38</sup> Consistent with the previous study, in our present study, we showed that the densities and frequencies of CD4<sup>+</sup>Foxp3<sup>+</sup> Treg cells were also significantly increased in intratumor TLSs than in peritumor TLSs in CRCLMs. Meanwhile, high level of Treg cells was negatively associated with T score and positively correlated with P score, which along with suppressive antitumor immune responses and poor prognosis. However, there have been few studies of the association between the density and frequency of macrophages in TLSs and CRCLM patients' prognosis. In the present study, we reported that the densities of CD68<sup>+</sup>CD163<sup>+</sup> M2 macrophages were significantly enriched in intratumor TLSs in CRCLMs and the frequencies of M2 macrophages were also negatively associated with T score and positively correlated with P score. Moreover, M2 macrophages promote tumor growth in the tumor microenvironment by inducing inflammation and angiogenesis, which lead to poor clinical outcomes.<sup>39–40</sup> In addition, Tfh and Treg cells have been reported to act in a complex balance in TLS formation and influence the composition of the neoplastic chronic inflammatory microenvironment.<sup>41</sup> Another study demonstrated that antigen-induced IL-2 production promoted the accumulation of Treg cells, and then contributed to the suppression of Th1-mediated adaptive immune responses. Subsequently, the IL-2-depleted microenvironment transformed some activated CD4<sup>+</sup> T cells into Tfh cells, which promoted the formation of TLSs and recruitment of tumor-infiltrating B cells.<sup>42</sup> Also, our present study showed that the densities of CD4<sup>+</sup>PD-1<sup>+</sup> Tfh cells were significantly increased in intratumor TLSs compared with peritumor TLSs, and thus promoting antitumor immune responses.

It is noteworthy that the density of each different type of cellular composition within TLSs was associated with patients' prognoses.<sup>43–44</sup> However, there is no established

immune classification of TLSs in CRCLM patients. Therefore, in our present study, an immune score that combines T score (intratumor TLSs) and P score (peritumor TLSs) was established and stratified CRCLM patients into four immune subclasses with significantly different clinical outcome. The immune class represented the distribution and abundance of TLSs in CRCLM tissues (figure 4G). Patients in immune class I have minimal intratumor TLSs and massive peritumor TLSs, indicating the least antitumor responses and poorest prognosis. On the contrary, patients in immune class IV have massive intratumor TLSs and minimal peritumor TLSs, indicating effective antitumor immune responses and longer survival. Immune class II and III represent patients with different distribution and abundance of TLSs in intratumor and peritumor, and thus these patients have different level of antitumor immune responses and prognoses. Furthermore, several studies demonstrated that the abundance of intratumor TLSs was associated with gene mutation, including BRAF.<sup>45–46</sup> In contrast, our study showed that common mutated genes in CRCLM, including BRAF and NRAS, have no significant association with intratumor and peritumor TLSs, which may have resulted from the different types of cancer. While intratumor and peritumor TLSs were clear prognostic indicator in this study, the standard methods for quantifying and characterizing them are highly labor intensive and pathologist-dependent. Clinical centers with advanced techniques could measure TLSs and conduct immune class system for wide-spread clinical utility, while clinical centers without advanced techniques could measure and characterize TLSs in morphology for clinical utility.

Furthermore, several recent studies reported that immune classification has been proposed for clinical practice in gastric cancer, CRC and CRCLM, with better predictive ability than prediction based on traditional clinical methods, including the CRS.<sup>47–49</sup> Consistent with previous findings, our study demonstrated that immune class, outperforming the CRS, was a novel system that would improve personalized surveillance, potentially assist clinical practice and enhance prognostic efficacy for CRCLM patients. However, several phenomena and mechanisms need to be further explored. First, as all retrospective studies have inherent limitations,<sup>50</sup> prospective clinical trials should be required to investigate the predictive power of using immune class as a biomarker for CRCLM patients who may be more responsive to immunotherapy. Second, the mechanisms that cause different distribution and abundance of TLSs in intratumor and peritumor region need to be further clarified. Third, TLS maturation is an important parameter of tumor immune contexture and bears significant prognostic and potential predictive value in CRC.<sup>43</sup> However, our study demonstrates no significant prognostic value of TLS maturation in CRCLM, which should be further verify by a cohort study with larger number of samples. Fourthly, the association between MSI status and immune cell infiltration in intratumor and peritumor region also need to be

further elucidated. Finally, in the tumor progression, it is necessary to further investigate whether the cellular components of TLSs are changed, and whether external intervention could regulate the cellular components of TLSs to enhance the antitumor immune responses.

## Conclusion

In conclusion, our present study demonstrated that the distribution and abundance of TLSs closely correlated with molecular subtype and survival of CRCLM patients, and a novel immune class was proposed for predicting the prognosis of CRCLM patients. Noticeably, we also showed that the specific cellular composition of TLSs would affect prognosis of CRCLM patients, especially, including Treg cells, M2 macrophages and Tfh cell, which could be used for improving the response level of clinical immunotherapy.

## Author affiliations

<sup>1</sup>Department of General Surgery, The First Affiliated Hospital of Anhui Medical University, Hefei, Anhui, China

<sup>2</sup>Department of General Surgery, Huashan Hospital Fudan University, Shanghai, China

<sup>3</sup>Department of General Surgery, Shanghai Tenth People's Hospital of Tongji University, Shanghai, China

<sup>4</sup>School of Pharmacy, Anhui Medical University, Hefei, China

<sup>5</sup>Inflammation and Immune Mediated Diseases Laboratory of Anhui Province, Anhui Medical University, Hefei, Anhui, China

<sup>6</sup>Department of Pathology, Huashan Hospital Fudan University, Shanghai, China

<sup>7</sup>Department of Pathology, The First Affiliated Hospital of Anhui Medical University, Hefei, Anhui, China

**Acknowledgements** Our special acknowledgments to Dr. Laura Jordhen (Department of Family Medicine, Landmark Health, Washington, USA) for revising the language of our manuscript.

**Contributors** CZ, X-YW, J-LZ and J-HC performed study concept and design. CZ, X-YW, J-LZ, BZ, Y-TL, C-HY, PZ, X-CM, Z-MC, YM, J-HH, B-RT, RZ, T-QW, LT, WG, S-YW, X-FZ, W-KY, Z-JK and X-WF performed acquisition of data. CZ, X-FW, X-WF, JF and X-YH performed analysis and interpretation of data. CZ, X-YW and J-LZ performed statistical analysis. CZ, X-YW and J-HC performed drafting of manuscript. J-HC, CZ and JL performed review and revision of the paper. J-HC, CZ and JL are responsible for the overall content as guarantor. All authors read and approved the final paper.

**Funding** This work was supported by the Clinical Research Project of the First Affiliated Hospital of Anhui Medical University (Grant nos LCYJ2021YB014), the University Research Project of Anhui Province (Grant nos 2022AH040161) and the Program of Shanghai Academic/Technology Research Leader (Grant nos 22XD1400300).

**Competing interests** No, there are no competing interests.

**Patient consent for publication** Not applicable.

**Ethics approval** Informed consent was provided by all patients, and the Ethical Committee of Huashan Hospital Fudan University (Shanghai, China) (ID: KY2022-946), Tenth People's Hospital of Tongji University (Shanghai, China) (ID: SHSY-IEC-5.0/22K296/P01) and the First Affiliated Hospital of Anhui Medical University (Anhui, China) (ID: Quick-PJ 2022-14-33).

**Provenance and peer review** Not commissioned; externally peer reviewed.

**Data availability statement** All data relevant to the study are included in the article or uploaded as online supplemental information.

**Supplemental material** This content has been supplied by the author(s). It has not been vetted by BMJ Publishing Group Limited (BMJ) and may not have been peer-reviewed. Any opinions or recommendations discussed are solely those of the author(s) and are not endorsed by BMJ. BMJ disclaims all liability and responsibility arising from any reliance placed on the content. Where the content includes any translated material, BMJ does not warrant the accuracy and reliability

of the translations (including but not limited to local regulations, clinical guidelines, terminology, drug names and drug dosages), and is not responsible for any error and/or omissions arising from translation and adaptation or otherwise.

**Open access** This is an open access article distributed in accordance with the Creative Commons Attribution Non Commercial (CC BY-NC 4.0) license, which permits others to distribute, remix, adapt, build upon this work non-commercially, and license their derivative works on different terms, provided the original work is properly cited, appropriate credit is given, any changes made indicated, and the use is non-commercial. See <http://creativecommons.org/licenses/by-nc/4.0/>.

## ORCID iD

Jin-Hong Chen <http://orcid.org/0000-0003-0952-9990>

## REFERENCES

- Sung H, Ferlay J, Siegel RL, *et al.* Global cancer statistics 2020: GLOBOCAN estimates of incidence and mortality worldwide for 36 cancers in 185 countries. *CA Cancer J Clin* 2021;71:209–49.
- Zhang C, Wang X-Y, Zhang P, *et al.* Cancer-Derived exosomal HSPC111 promotes colorectal cancer liver metastasis by reprogramming lipid metabolism in cancer-associated fibroblasts. *Cell Death Dis* 2022;13:57.
- Zhang C, Wang X, Han J, *et al.* Histological tumor response to neoadjuvant chemotherapy correlates to immunoscore in colorectal cancer liver metastases patients. *J Surg Oncol* 2021;124:1431–41.
- Han J, Wang X, Zhang C, *et al.* Clinicopathological and prognostic significance of HER2 status in surgically resected colorectal liver metastases. *J Surg Oncol* 2022;125:991–1001.
- Zhang C, Wang L, Jin C, *et al.* Long non-coding RNA Inc-LALC facilitates colorectal cancer liver metastasis via epigenetically silencing LZTS1. *Cell Death Dis* 2021;12:224.
- Van Cutsem E, Nordlinger B, Adam R, *et al.* Towards a pan-European consensus on the treatment of patients with colorectal liver metastases. *Eur J Cancer* 2006;42:2212–21.
- Lintoiu-Ursut B, Tulin A, Constantinoiu S. Recurrence after hepatic resection in colorectal cancer liver metastasis -review article-. *J Med Life* 2015;8:12–4.
- Moretto R, Corallo S, Belfiore A, *et al.* Prognostic impact of immune-microenvironment in colorectal liver metastases resected after triplets plus a biologic agent: a pooled analysis of five prospective trials. *Eur J Cancer* 2020;135:78–88.
- Liu Y, Zhang Q, Xing B, *et al.* Immune phenotypic linkage between colorectal cancer and liver metastasis. *Cancer Cell* 2022;40:424–37.
- Xu Y, Wei Z, Feng M, *et al.* Tumor-infiltrated activated B cells suppress liver metastasis of colorectal cancers. *Cell Rep* 2022;40:S2211-1247(22)01115-9:111295..
- Ansell SM, Lesokhin AM, Borrello I, *et al.* Pd-1 blockade with nivolumab in relapsed or refractory Hodgkin's lymphoma. *N Engl J Med* 2015;372:311–9.
- Check JH, Dix E, Sansoucie L. Support for the hypothesis that successful immunotherapy of various cancers can be achieved by inhibiting a progesterone associated immunomodulatory protein. *Med Hypotheses* 2009;72:87–90.
- Fridman WH, Zitvogel L, Sautès-Fridman C, *et al.* The immune contexture in cancer prognosis and treatment. *Nat Rev Clin Oncol* 2017;14:717–34.
- Oshi M, Kawaguchi T, Yan L, *et al.* Immune cytolytic activity is associated with reduced intra-tumoral genetic heterogeneity and with better clinical outcomes in triple negative breast cancer. *Am J Cancer Res* 2021;11:3628–44.
- Engelhard VH, Rodriguez AB, Mauldin IS, *et al.* Immune cell infiltration and tertiary lymphoid structures as determinants of antitumor immunity. *J Immunol* 2018;200:432–42.
- Sautès-Fridman C, Lawand M, Giraldo NA, *et al.* Tertiary lymphoid structures in cancers: prognostic value. *Regulation, and Manipulation for Therapeutic Intervention Front Immunol* 2016;7:407.
- Fridman WH, Pagès F, Sautès-Fridman C, *et al.* The immune contexture in human tumours: impact on clinical outcome. *Nat Rev Cancer* 2012;12:298–306.
- Calderaro J, Petitprez F, Becht E, *et al.* Intra-tumoral tertiary lymphoid structures are associated with a low risk of early recurrence of hepatocellular carcinoma. *J Hepatol* 2019;70:58–65.
- Petitprez F, de Reyniès A, Keung EZ, *et al.* B cells are associated with survival and immunotherapy response in sarcoma. *Nature* 2020;577:556–60.
- Helmsink BA, Reddy SM, Gao J, *et al.* B cells and tertiary lymphoid structures promote immunotherapy response. *Nature* 2020;577:549–55.



- 21 Sautès-Fridman C, Petitprez F, Calderaro J, *et al.* Tertiary lymphoid structures in the era of cancer immunotherapy. *Nat Rev Cancer* 2019;19:307–25.
- 22 Fong Y, Fortner J, Sun RL, *et al.* Clinical score for predicting recurrence after hepatic resection for metastatic colorectal cancer: analysis of 1001 consecutive cases. *Ann Surg* 1999;230:309–18;
- 23 Murakami J, Shimizu Y, Kashii Y, *et al.* Functional B-cell response in intrahepatic lymphoid follicles in chronic hepatitis C. *Hepatology* 1999;30:143–50.
- 24 Oba M, Nakanishi Y, Amano T, *et al.* Stratification of postoperative prognosis by invasive tumor thickness in perihilar cholangiocarcinoma. *Ann Surg Oncol* 2021;28:2001–9.
- 25 Huang Y-K, Wang M, Sun Y, *et al.* Macrophage spatial heterogeneity in gastric cancer defined by multiplex immunohistochemistry. *Nat Commun* 2019;10:3928.
- 26 Moosavi SH, Eide PW, Eilertsen IA, *et al.* De novo transcriptomic subtyping of colorectal cancer liver metastases in the context of tumor heterogeneity. *Genome Med* 2021;13:143.
- 27 N J, J T, SI N, *et al.* Tertiary lymphoid structures and B lymphocytes in cancer prognosis and response to immunotherapies. *Oncoimmunology* 2021;10:1900508.
- 28 Sinha N, Sinha S, Valero C, *et al.* Immune determinants of the association between tumor mutational burden and immunotherapy response across cancer types. *Cancer Res* 2022;82:2076–83.
- 29 Aoki T, Chong LC, Takata K, *et al.* Single-Cell transcriptome analysis reveals disease-defining T-cell subsets in the tumor microenvironment of classic Hodgkin lymphoma. *Cancer Discov* 2020;10:406–21.
- 30 Hinshaw DC, Shevde LA. The tumor microenvironment innately modulates cancer progression. *Cancer Res* 2019;79:4557–66.
- 31 Jenkins MA, Hayashi S, O'Shea A-M, *et al.* Pathology features in Bethesda guidelines predict colorectal cancer microsatellite instability: a population-based study. *Gastroenterology* 2007;133:48–56.
- 32 Rozek LS, Schmit SL, Greenson JK, *et al.* Tumor-Infiltrating lymphocytes, crohn's-like lymphoid reaction, and survival from colorectal cancer. *J Natl Cancer Inst* 2016;108:djw027.
- 33 Chang EY, Dorsey PB, Frankhouse J, *et al.* Combination of microsatellite instability and lymphocytic infiltrate as a prognostic indicator in colon cancer. *Arch Surg* 2009;144:511–5.
- 34 Fink S, Yuan D, Stein I, *et al.* Ectopic lymphoid structures function as microniches for tumor progenitor cells in hepatocellular carcinoma. *Nat Immunol* 2015;16:1235–44.
- 35 Noël G, Fontsa ML, Garaud S, *et al.* Functional th1-oriented T follicular helper cells that infiltrate human breast cancer promote effective adaptive immunity. *J Clin Invest* 2021;131:e139905.
- 36 Choi J, Diao H, Faliti CE, *et al.* Bcl-6 is the nexus transcription factor of T follicular helper cells via repressor-of-repressor circuits. *Nat Immunol* 2020;21:777–89.
- 37 Azizov V, Dietel K, Steffen F, *et al.* Ethanol consumption inhibits Tfh cell responses and the development of autoimmune arthritis. *Nat Commun* 2020;11:1998.
- 38 Li H, Wang J, Liu H, *et al.* Existence of intratumoral tertiary lymphoid structures is associated with immune cells infiltration and predicts better prognosis in early-stage hepatocellular carcinoma. *Aging (Albany NY)* 2020;12:3451–72.
- 39 Poh AR, Ernst M. Targeting macrophages in cancer: from bench to bedside. *Front Oncol* 2018;8:49.
- 40 Nakayama T, Sugano Y, Yokokawa T, *et al.* Clinical impact of the presence of macrophages in endomyocardial biopsies of patients with dilated cardiomyopathy. *Eur J Heart Fail* 2017;19:490–8.
- 41 Rossi A, Belmonte B, Carnevale S, *et al.* Stromal and immune cell dynamics in tumor associated tertiary lymphoid structures and anti-tumor immune responses. *Front Cell Dev Biol* 2022;10:933113.
- 42 Gu-Trantien C, Loi S, Garaud S, *et al.* CD4(+) follicular helper T cell infiltration predicts breast cancer survival. *J Clin Invest* 2013;123:67428:2873–92..
- 43 Posch F, Silina K, Leibl S, *et al.* Maturation of tertiary lymphoid structures and recurrence of stage II and III colorectal cancer. *Oncoimmunology* 2018;7:e1378844.
- 44 Lauss M, Donia M, Svane IM, *et al.* B cells and tertiary lymphoid structures: friends or foes in cancer immunotherapy? *Clin Cancer Res* 2022;28:1751–8.
- 45 Yu J-S, Huang W-B, Zhang Y-H, *et al.* The association of immune cell infiltration and prognostic value of tertiary lymphoid structures in gastric cancer. *Neoplasma* 2022;69:886–98.
- 46 Ding G-Y, Ma J-Q, Yun J-P, *et al.* Distribution and density of tertiary lymphoid structures predict clinical outcome in intrahepatic cholangiocarcinoma. *J Hepatol* 2022;76:608–18.
- 47 Li J, Pu K, Li C, *et al.* A novel six-gene-based prognostic model predicts survival and clinical risk score for gastric cancer. *Front Genet* 2021;12:615834.
- 48 Katz SC, Bamboat ZM, Maker AV, *et al.* Regulatory T cell infiltration predicts outcome following resection of colorectal cancer liver metastases. *Ann Surg Oncol* 2013;20:946–55.
- 49 Miao YD, Wang JT, Yang Y, *et al.* Identification of prognosis-associated immune genes and exploration of immune cell infiltration in colorectal cancer. *Biomark Med* 2020;14:1353–69.
- 50 Iorgulescu JB, Gokhale PC, Speranza MC, *et al.* Concurrent dexamethasone limits the clinical benefit of immune checkpoint blockade in glioblastoma. *Clin Cancer Res* 2021;27:276–87.